CHAPTER IV

RESULTS AND DISCUSSION

4.1 Alternative Layer-by-layer Adsorption of Poly(styrene sulfonate) and Chitosan

Multilayer film on amino-containing substrate was prepared by alternative adsorption between poly(styrene sulfonate) (PSS) and chitosan (CHI) having molecular weight of 70,000 and 150,000, respectively. A number of adsorption variables were investigated and used to control the thickness of each layer and overall assembled layer. The thickness of adsorbed layer was monitored by ellipsometry.

4.1.1 Preparation of Amino-containing Substrate

The substrates used for all experiments were silicon oxide substrates that were chemically modified to incorporate amine functionality in its surface region. Silicon oxide reacts with 1% of 3-amino(propyl triethoxysilane) (APTES) to form amine-functionalized surface (Si-NH_2). The condition chosen in this experiment yielded a surface containing a ~ 63 ± 10 Å thick modified layer.

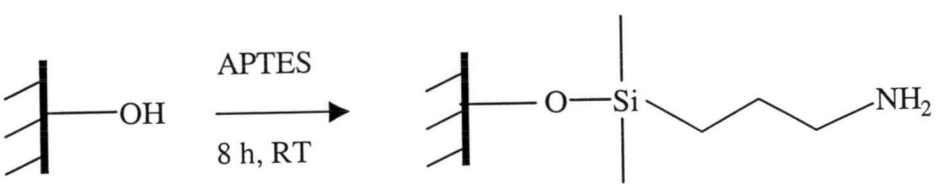

Scheme 4.1 Reaction between a silicon oxide substrate and APTES.

4.1.2 Multilayer Formation

PSS can be easily soluble in water. Since PSS is a strong polyelectrolyte ,sulfonic acid groups on the polymer backbone ($-SO_3H$) are completely dissociated into negatively charge of sulfonate groups ($-SO_3^-$) in the working pH range (1-14). On the other hand, CHI is only soluble in acidic solution so the polymer backbone bears positively charge of ammonium groups ($-NH_3^+$) when pH is below 5. Multilayer formation was thus carried out at pH 4, the pH at which PSS is in the form of negatively charged polyelectrolyte while CHI is in the form of positively charged polyelectrolyte. Due to the positive nature of amino groups on the amine-functionalized substrate, PSS was used as the first layer to be adsorbed. If the total number of layer is odd, the last layer adsorbed is PSS. If the total number of layer is even, the last layer adsorbed is CHI. The adsorbed multilayer using different condition was compared in the term of average bilayer thickness. Up to 20 layers were assembled for each condition.

4.1.2.1. Effect of Chitosan Concentration

The first adsorption parameter to be determined was polymer concentration. The average bilayer thickness of the multilayer films using various chitosan concentrations is shown in Figure 4.2. The film thickness of bilayer was quite independent of chitosan concentration in the range of 0.25-1.0 mg/mL. The experiments were carried out in the presence of 0.25 M NaCl. This set of data indicated that polymer concentration did not significantly affect the layer thickness presumably due to the fact that this particular range of concentration is on the plateau region of adsorption isotherm of CHI on Si-NH_2-PSS. PSS concentration used in the layer assembly was fixed at 3 mg/mL. It was believed that this concentration was sufficiently high for the adsorption of PSS to reach its equilibrium.

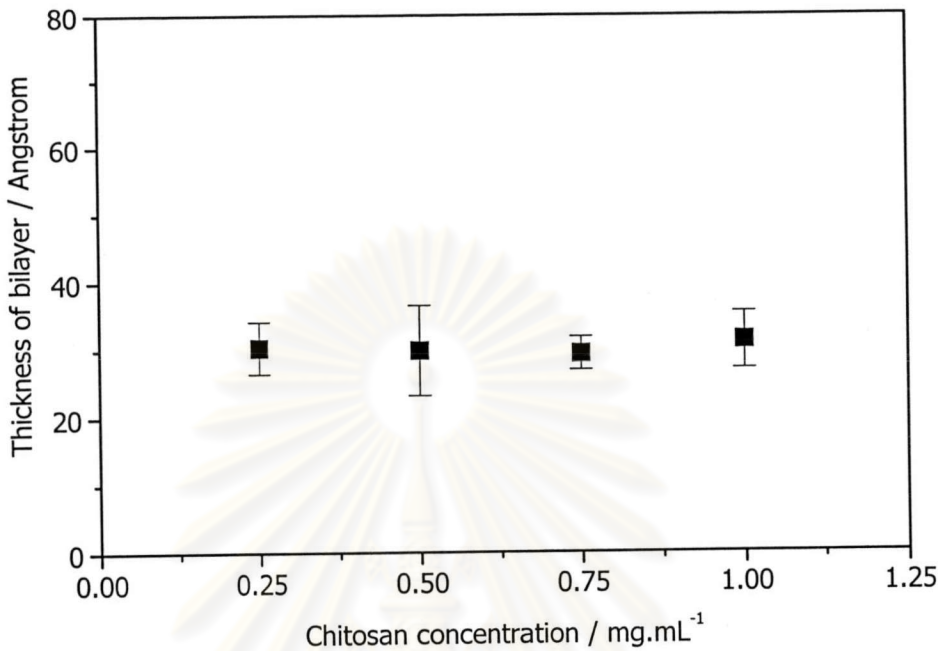

Figure 4.1 The average thickness of PSS-CHI bilayer calculated from ellipsometric data of Si-NH_2-$(PSS\text{-}CHI)_5$ assemblies as a function of chitosan concentration in the presence of 0.25 M NaCl.

4.1.2.2 Effect of Ionic Strength

The ionic strength of polymer solution was varied by an addition of NaCl. The average thickness of bilayer was plotted as a function of NaCl concentration in Figure 4.2. The average thickness of bilayer assemblies were 18, 30, 36 and 42 Å, when 0, 0.25, 0.5 and 1 M of NaCl was incorporated in chitosan solution, respectively. This result suggested that the amount of polymer adsorbed gradually increased as the amount of NaCl increased. This can be explained by the fact that the coiled polymer can adsorb more in the presence of NaCl due to a relaxation of electrostatic repulsion in polymer solution. Random coil can obviously result in thicker individual layer and multilayers as compared with loop and train, dominated conformations of polymer chains in the absence of NaCl.

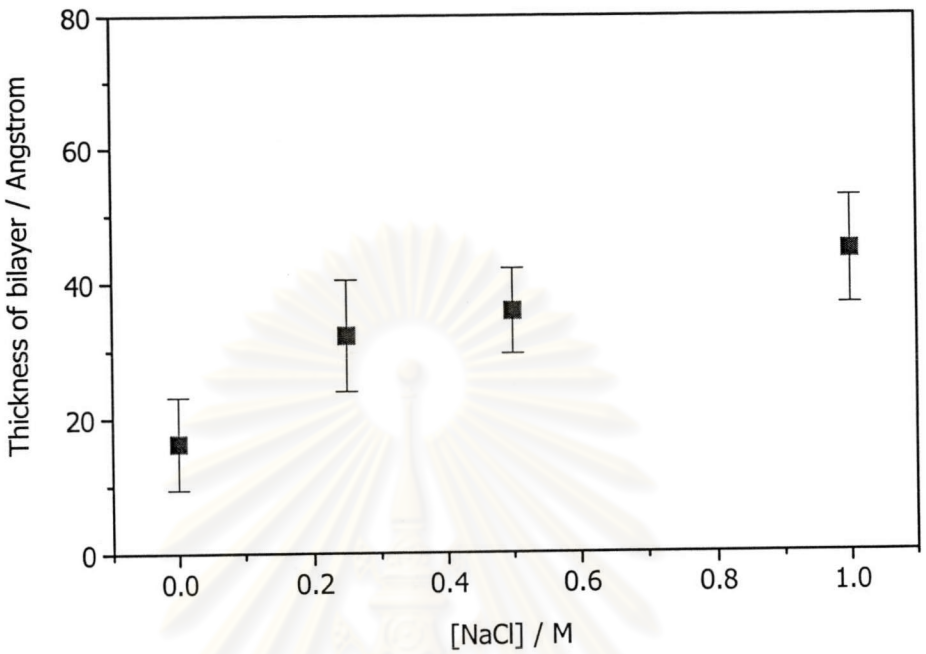

Figure 4.2 The average thickness of PSS-CHI bilayer calculated from ellipsometric data of Si-NH_2-$(PSS\text{-}CHI)_{10}$ assemblies as a function of NaCl concentration.

Figure 4.3 displays a continuous increase of the thickness with the number of layer for all conditions, indicating a stepwise polymer deposition. The addition of NaCl into PSS solution seems to have a stronger influence on overall multilayer thickness as compared with the previous condition of which NaCl was only added to CHI solution. This may be due to the fact that a thicker PSS layer adsorbed as the first layer induced more CHI to adsorb. The magnitude of thickness progression was enhanced even more when NaCl was incorporated into both PSS and CHI solutions. The average thickness of bilayer assemblies were 18 Å in the absence of NaCl and 30, 37 and 59 Å, when 0.25 M NaCl was added in CHI, PSS and in both PSS and CHI solutions, respectively. The thickness of an initial bilayer is clearly a critical parameter that controls overall multilayer thickness.

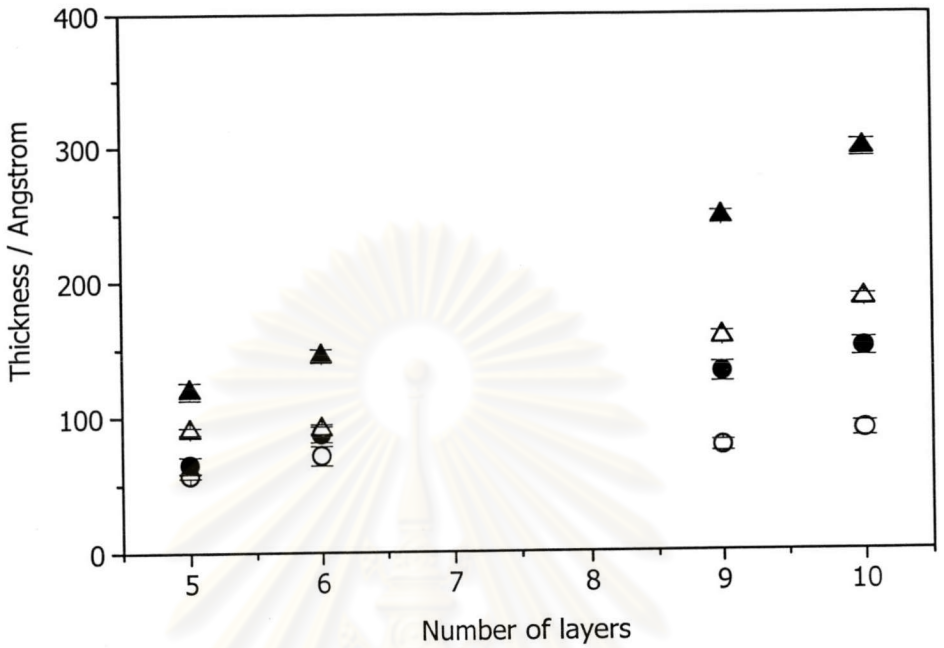

Figure 4.3 Ellipsometric thickness of Si-NH_2-$(PSS\text{-}CHI)_n$ assemblies as a function of the number of layer; no NaCl (○), 0.25 M NaCl in CHI solution (●), 0.25 M NaCl in PSS solution (Δ), 0.25 M NaCl in both CHI and PSS solutions (▲).

4.1.3 Confirmation of Layer Formation by ATR-IR and XPS

X-ray photoelectron spectroscopy was used to confirm the layer formation by monitoring the atomic composition before and after multilayer assembly. As shown in Figure 4.4, the appearance of N_{1s} verifies the success of chemical modification of silicon oxide surface with APTES. The signals of S_{1s} appearing on Figure 4.5 indicated the existence of PSS in the multilayer film. The attenuation of the signal from Si_{2p} suggested that the thickness of 10 bilayers of $(PSS\text{-}CHI)_{10}$ on Si-NH_2 should be thicker than the XPS sampling (~ 50 Å). The speculation was later proved by ellipsometry that thickness of 10 bilayers of $(PSS\text{-}CHI)_{10}$ was 45 Å. This multilayer film was prepared in the presence of 1 M NaCl. A stoichiometric ratio of N:S was 4 : 1 indicating an excess of CHI when it was the top layer.

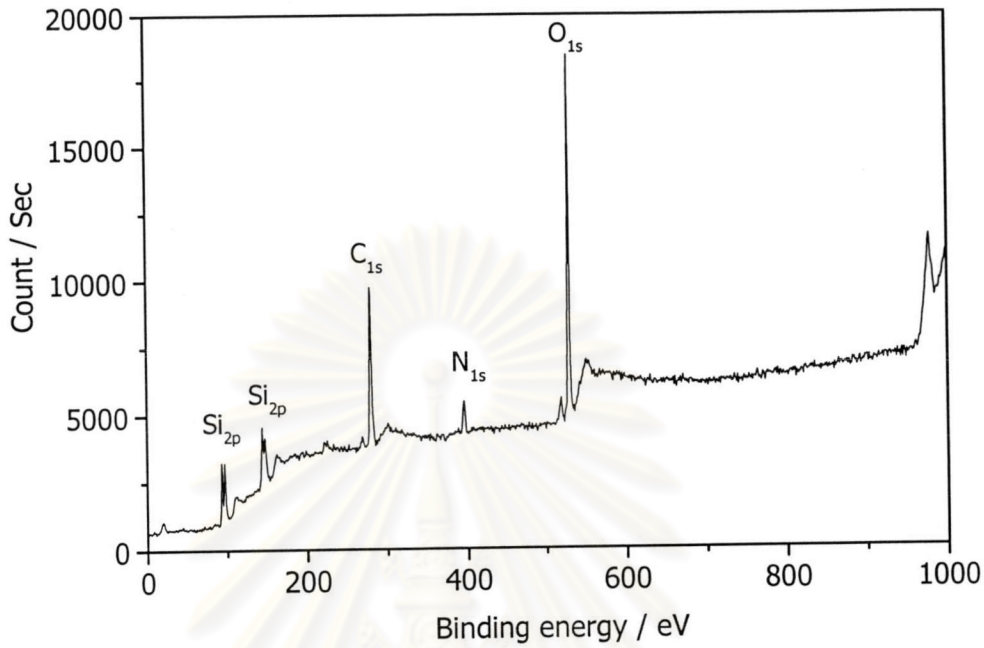

Figure 4.4. XPS survey spectrum of Si-NH_2 substrate.

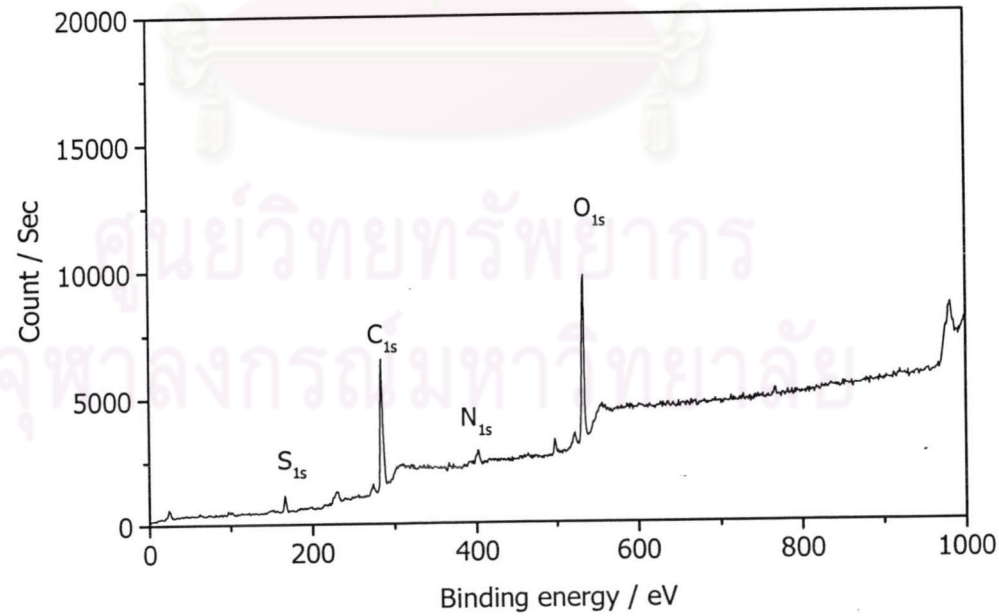

Figure 4.5 XPS survey spectrum of Si-NH_2-(PSS-CHI)$_{10}$.

Table 4.1 Atomic composition of Si-NH_2 substrate and Si-NH_2-$(PSS\text{-}CHI)_{10}$.

Sample	Atomic composition (%)				
	C	O	Si	N	S
Si-NH_2	33.37	22.97	25.04	18.62	0.00
Si-NH_2-$(PSS\text{-}CHI)_{10}$	55.32	22.28	0.00	18.09	4.32

In addition, ATR-IR was used to characterize functional groups of multilayer films. Due to the limitation of ATR-IR technique for analyzing multilayers assembled on brittle substrate of Si-NH_2, commercial plasma-treated poly(ethylene terephthalate) (PET) was introduced as an alternative substrate which is more flexible and easy to handle. The surface of plasma-treated PET is hydrophilic and bears some polar functionalities such as hydroxyl and carboxylic acid groups. It is thus capable of forming multilayer assembly. At pH 4, the treated PET should be able to adsorb CHI via electrostatic interaction ($-COO^-$ with $-NH_3^+$) in combination with hydrogen bonding (-OH with $-NH_3^+$). The layer-by-layer deposition was carried out in the presence of 1 M NaCl. ATR-IR spectrum of PET-$(CHI\text{-}PSS)_{14}$-CHI assembly is shown in Figure 4.6. The broad peak in the range of 2500-3700 cm^{-1} can be assigned to the overlapping between N-H stretching and O-H stretching which belong to CHI and PSS, respectively. The existing of PSS was also demonstrated by S=O stretching in the range of 1050-1200 cm^{-1}. As evidenced in Figure 4.7, a continuous increase of absorbance as a function of the number of layer implied that ATR-IR technique can be used as a tool to qualitatively monitor the multilayer assembly.

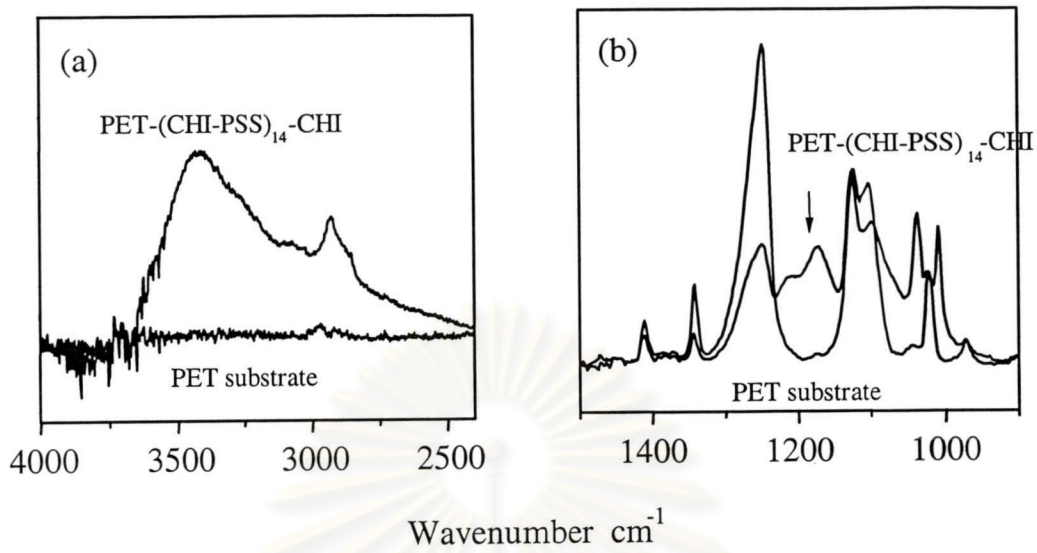

Figure 4.6. ATR-IR spectra of PET and PET-(CHI-PSS)$_{14}$-CHI assemblies; (a) O-H and N-H stretching (b) S=O stretching.

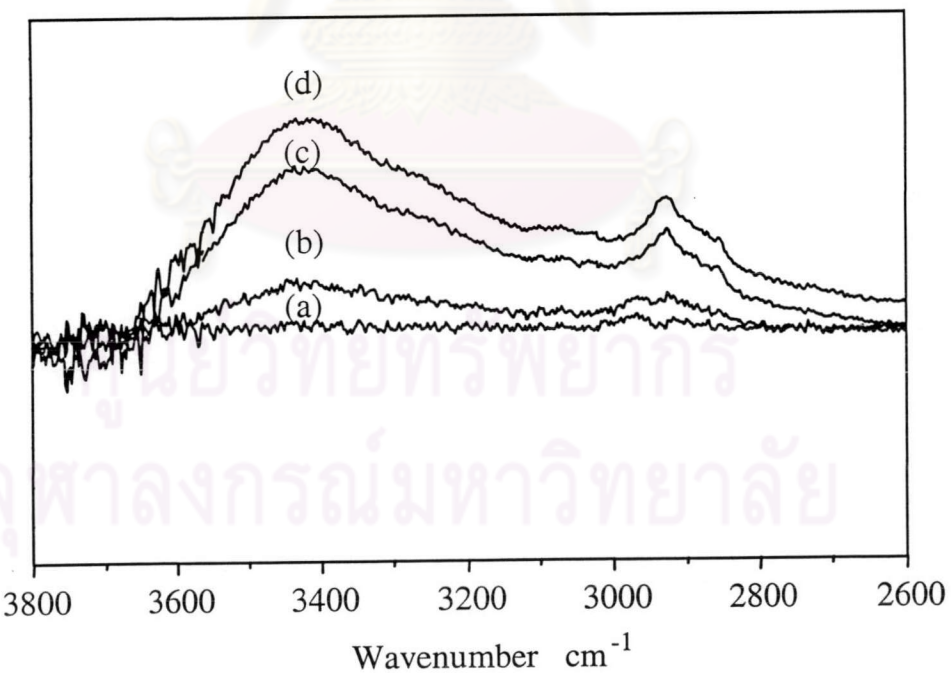

Figure 4.7 ATR-IR spectra of PET-(CHI-PSS)$_n$ assembly; (a) PET, (b) PET-(CHI-PSS)$_4$-CHI, (c) PET-(CHI-PSS)$_9$-CHI, (d) PET-(CHI-PSS)$_{14}$-CHI.

4.1.4 Stratification of Multilayer Film

4.1.4.1 Zeta-Potential

The measurement of zeta-potential was used to assess surface potential of the assembled film. If the concept of alternative adsorption is valid, the charge of deposited film should alternatively change between positive and negative depending upon the last layer deposited. In other words, the multilayer should be stratified. The surface potential should be negative and positive if PSS and CHI are the last layer deposited, respectively. The expected trend was observed in Figure 4.8 indicating that the multilayer was stratified and the charge was reversed after each deposition.

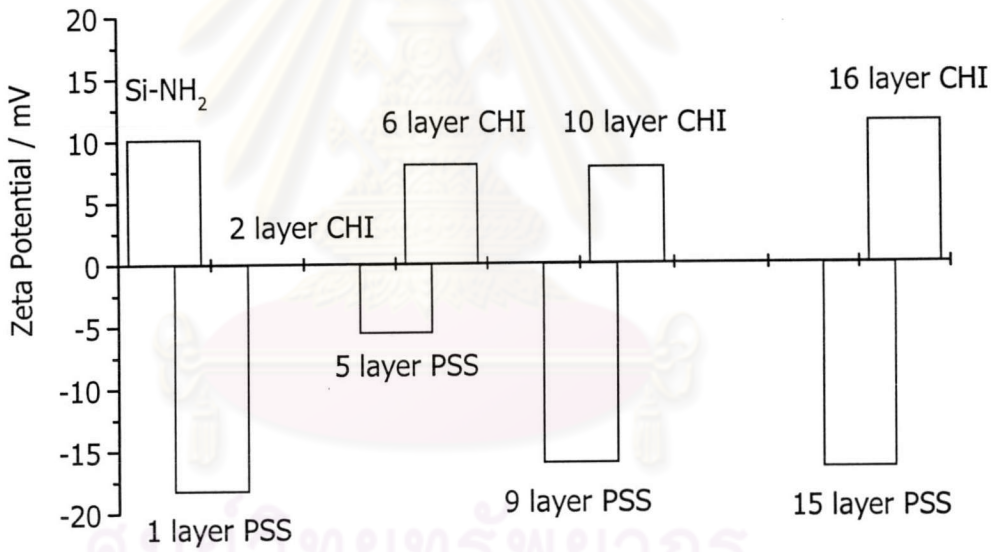

Figure 4.8 Zeta-potential of Si-NH_2-(PSS-CHI)$_n$ assemblies, 0.25 M NaCl was added to chitosan solution.

4.1.4.2 Water Contact Angle

The stratification of multilayer film can also be assessed by water contact angle measurements. The wettability should presumably be alternated depending upon which polymer was last deposited. As can be seen from Figure 4.9, the films having the odd number of layer (CHI is the top layer) were slightly more hydrophilic than the ones having the even number of layer (PSS is the top layer). This data also implied that each individual layer is thicker than the contact angle sampling depth so the surface wettability was then determined by the top layer.

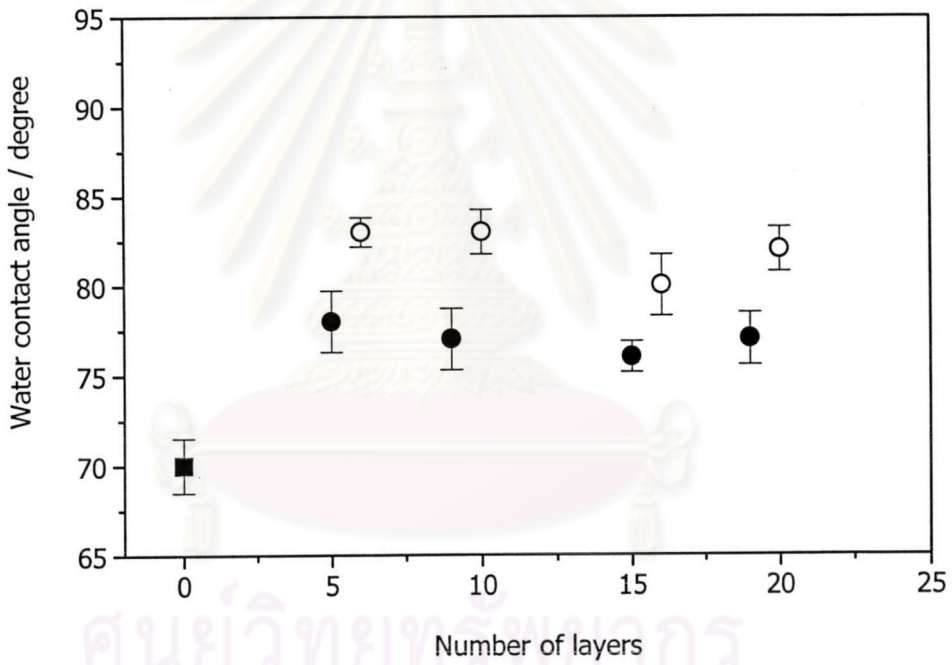

Figure 4.9 Water contact angle of Si-NH_2-$(PSS\text{-}CHI)_n$ assemblies, 0.25 M NaCl was added to chitosan solution; Si-NH_2 (■), odd layer (●), even layer (○).

4.1.5 Surface Topography of Multilayer Films

Atomic force microscopy (AFM) was used to investigate the surface topography of Si-NH_2-(PSS-CHI)$_n$ assembled films. The multilayer films were prepared either in the absence or in the presence of 1 M NaCl both in PSS and in CHI solutions. The R_a value reflects the average roughness of the whole image. The Si-NH_2 substrate showed a mean roughness of 0.5 nm indicating a relatively smooth surface (See Figure 4.10). The surface topography of multilayer films prepared in the absence and in the presence of 1M NaCl is shown in Figures 4.11 and 4.12, respectively. In the case of multilayer films prepared in the absence of NaCl, the surface appeared to be increasing in the roughness as the number of layer increased according to Figure 4.13. The surface roughness of multilayer films prepared in the presence of NaCl tended to reach the value of ~10 nm even at low number of layer and remained relatively constant up until 16 deposited layers. Eventhough multilayer films having 16 layers in both cases attained a similar value of R_a, their surface topographies appeared completely different. To better explain this result, it is necessary to take R_z into consideration. R_z represents the standard deviation of surface roughness. In other words, it indicates the height and depth fluctuation of each AFM images. As plotted in Figure 4.14, R_z seems to fluctuate quite a lot due to hills and valleys appearing on the image, especially when the film is quite thick. This fluctuation may disappear if the scan area is narrow down perhaps to 2x2 or 1x1 μm^2 Thus, it is much more reasonable to use both R_a and R_z to explain surface roughness and topography and taking into account the scan area of the samples.

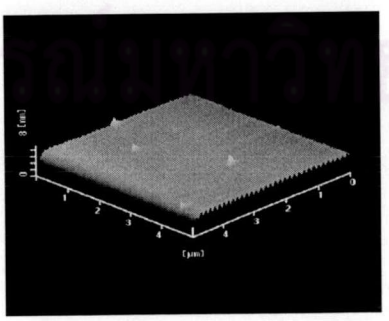

Figure 4.10 An AFM image (5x5μm^2) of Si-NH_2.

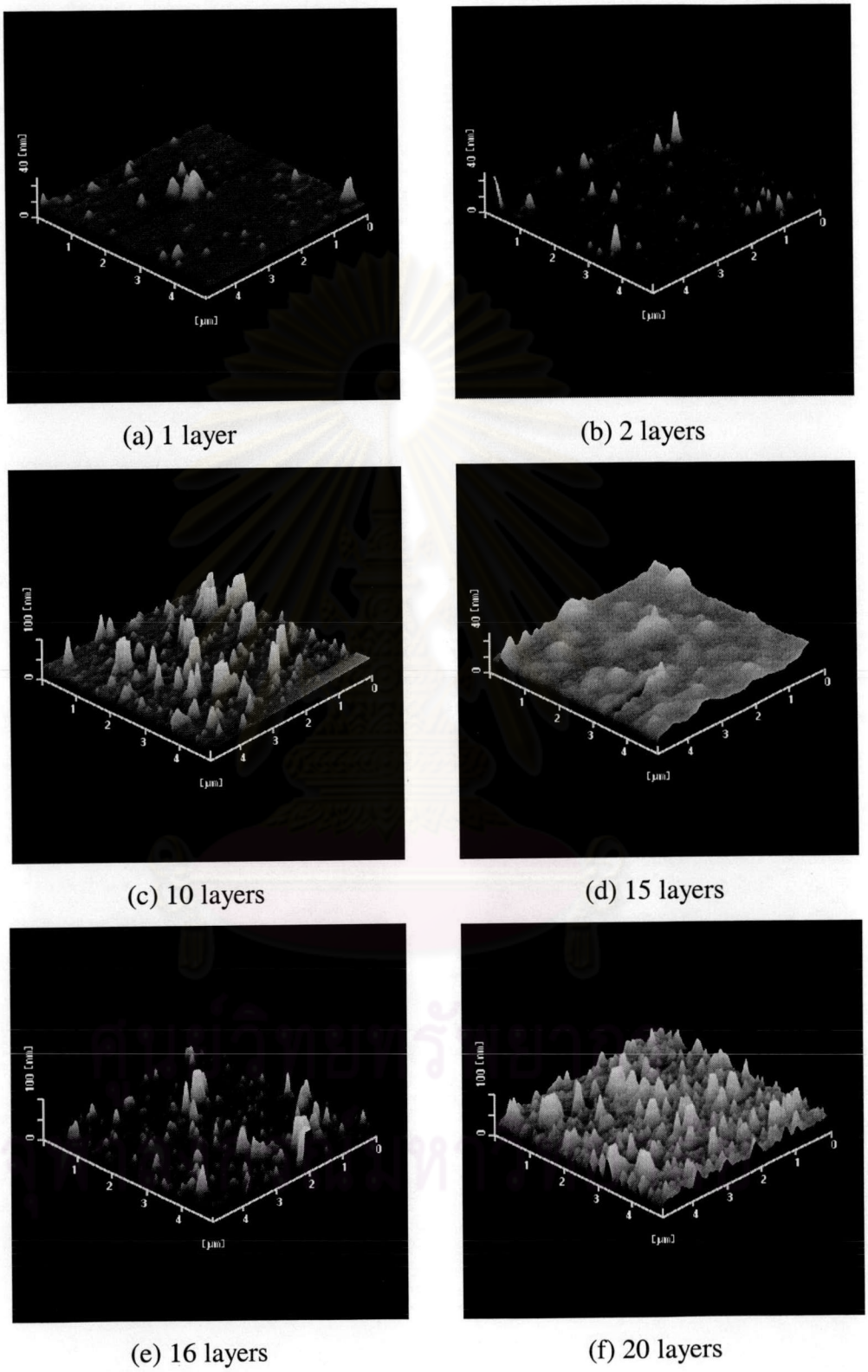

(a) 1 layer (b) 2 layers

(c) 10 layers (d) 15 layers

(e) 16 layers (f) 20 layers

Figure 4.11 AFM images ($5x5\mu m^2$) of Si-NH_2-$(PSS\text{-}CHI)_n$ prepared without 1 M NaCl; (a) 1 layer, (b) 2 layers, (c) 10 layers ,(d) 15 layers ,(e) 16 layers and (f) 20 layers.

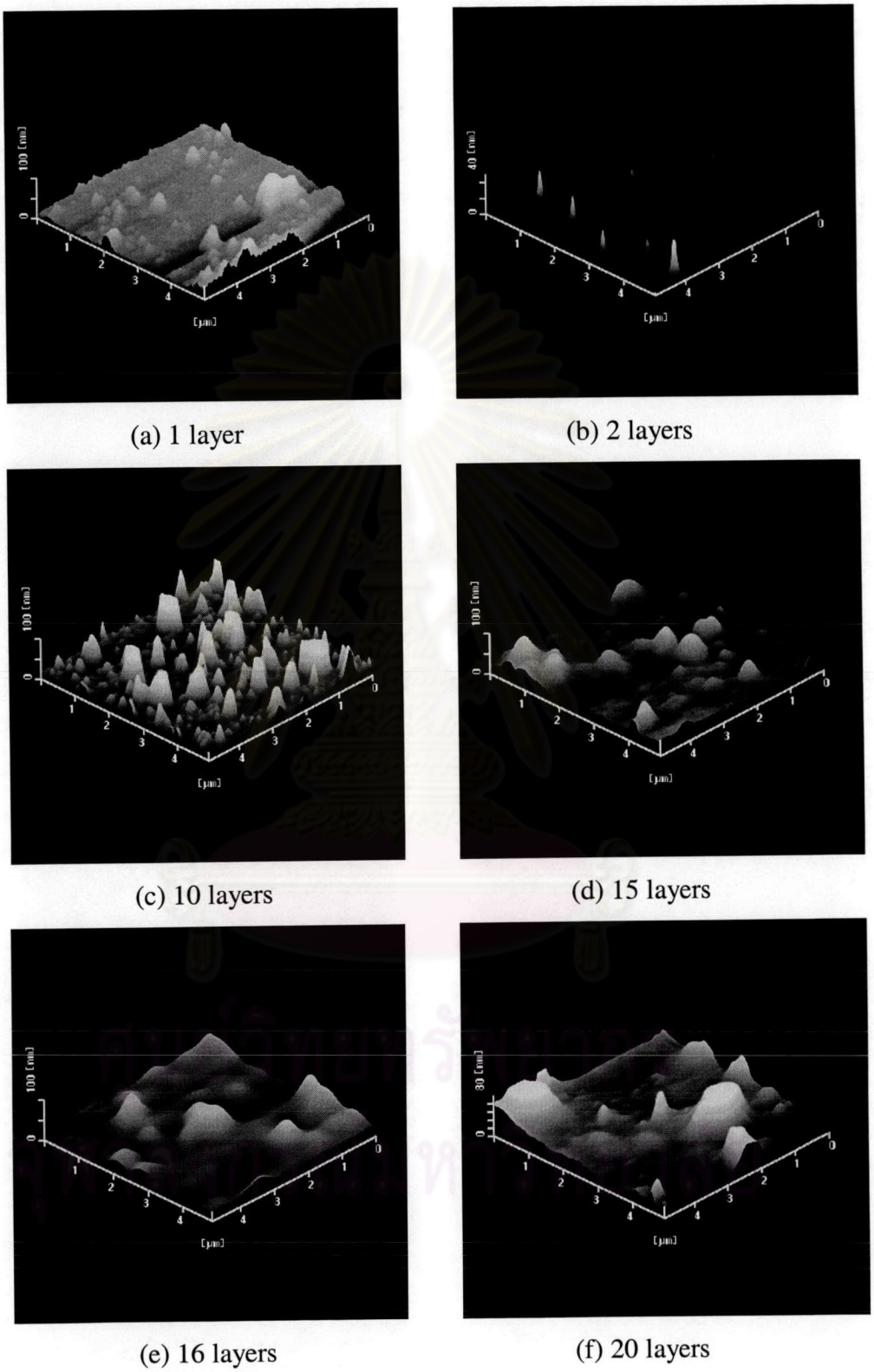

(a) 1 layer (b) 2 layers

(c) 10 layers (d) 15 layers

(e) 16 layers (f) 20 layers

Figure 4.12 AFM images ($5x5\mu m^2$) of Si-NH_2-$(PSS\text{-}CHI)_n$ prepared with 1 M NaCl; (a) 1 layer, (b) 2 layers, (c) 10 layers, (d) 15 layers ,(e) 16 layers and (f) 20 layers.

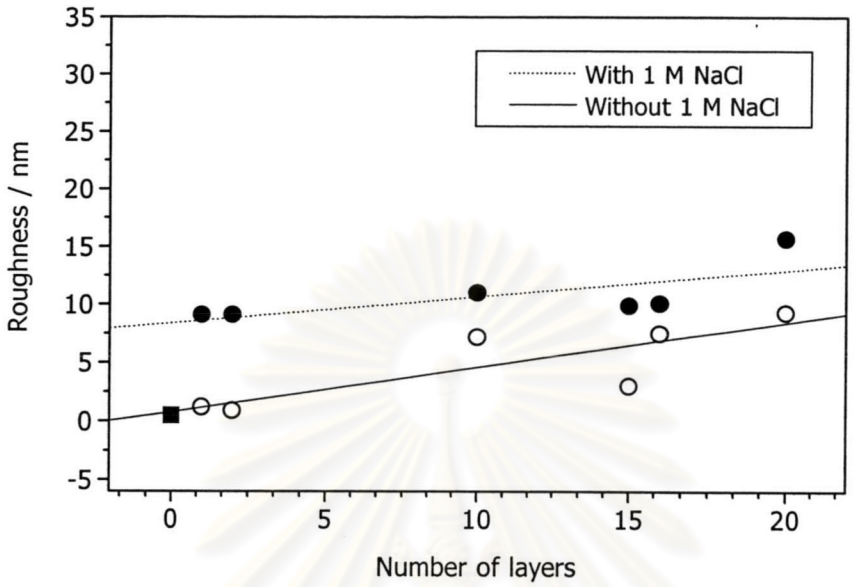

Figure 4.13 The surface roughness (R_a) of Si-NH_2-(PSS-CHI)$_n$ as a function of number of layers ; with 1M NaCl (●), without 1M NaCl (O) and Si-NH_2 layer (■).

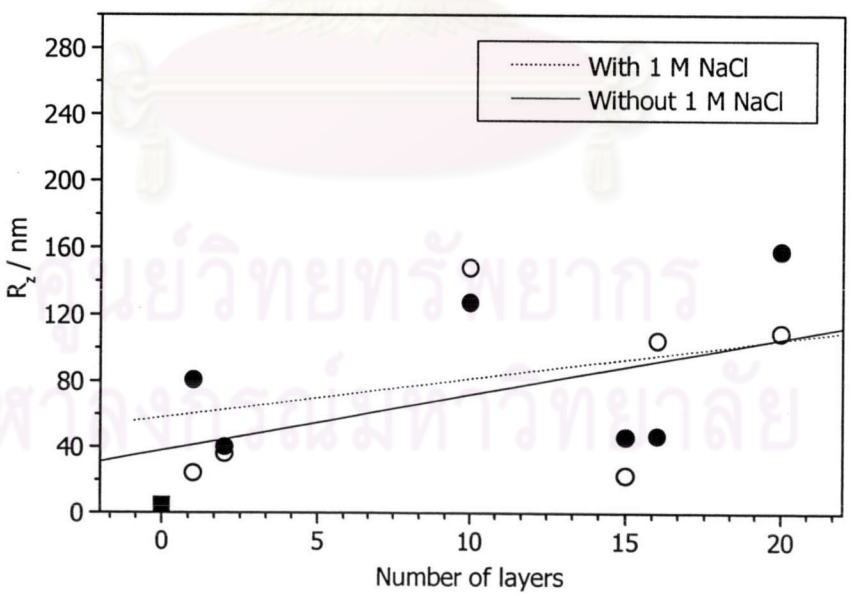

Figure 4.14 R_z value of Si-NH_2-(PSS-CHI)$_n$ as a function of number of layers ; with 1M NaCl (●), without 1M NaCl (O) and Si-NH_2 layer (■).

4.1.6 Blood Compatibility

In this study, the blood compatibility of multilayer films was determined with an attention to investigate the interaction between the surface and blood components which were, platelet-poor plasma (PPP) and platelet-rich plasma (PRP). In order to analyze the effects of the thickness of assembled film on blood compatibility, two conditions were chosen for multilayer film preparation. The samples prepared with or without 1M NaCl added in PSS and CHI solutions.

Plasma Protein Adsorption

The amount of plasma protein adsorbed on a material surface is a primary factor in evaluating the blood compatibility of the material. When polymeric biomaterial is in contact with blood, surface induced thrombosis is initated by the adsorption of plasma protein, followed by adhesion and activation of platelets. Here the amount of plasma protein adsorption using BCA microassay is determined. The calibration curve using albumin as a standard is displayed in Figure 4.15.

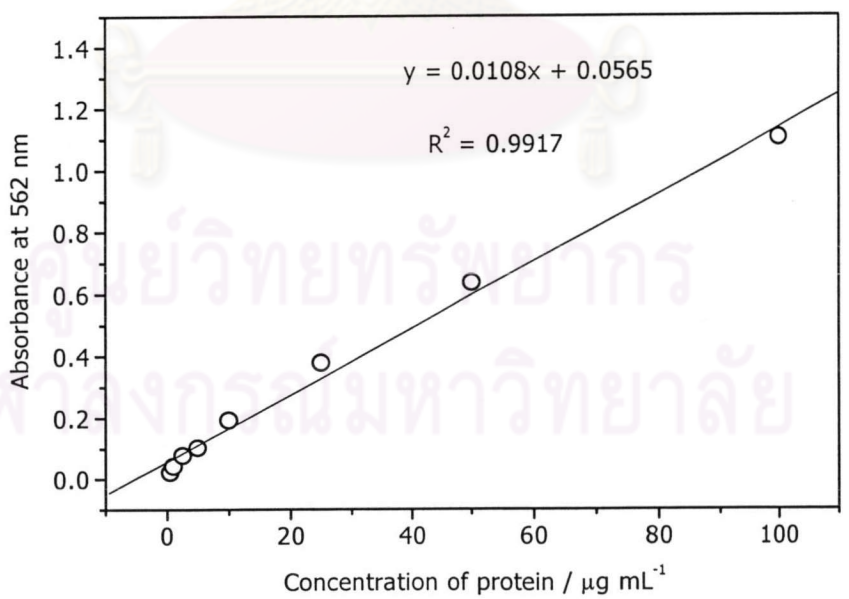

Figure 4.15 A calibration curve of the amount of albumin adsorbed and the absorbance obtained from BCA microassay.

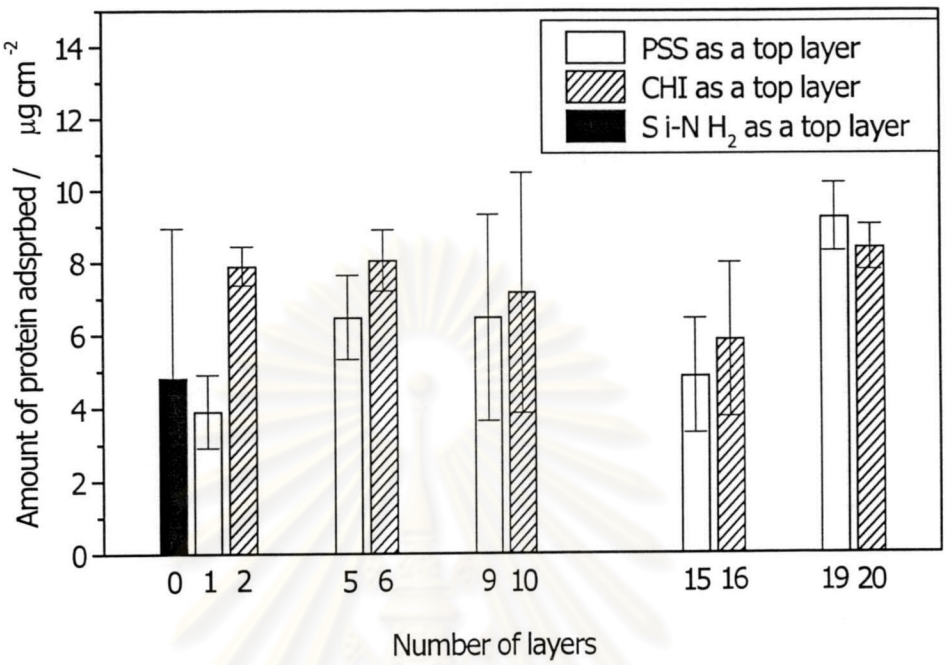

Figure 4.16 The amount of plasma protein adsorption per surface area ($\mu g/cm^2$) of $Si\text{-}NH_2\text{-}(PSS\text{-}CHI)_n$ assemblies prepared in the absence of NaCl.

Figure 4.16 shows the amount of plasma protein adsorbed on multilayer films prepared without NaCl. The amount of plasma protein adsorbed was slightly higher on the surface having CHI as the top layer as compared to the one having PSS as the top layer. This result indicated a strong electrostatic interaction between the positively charged chitosan and blood proteins carrying negative charges. Chitosan can induce the plasma protein adsorption whereas PSS can suppress protein adsorption. The alternative trend was observed up to 16 layers. The amount of protein adsorbed on the 19-layer film having PSS as the top layer became higher than the one on the 16-layer film eventhough its surface charge is negative. This observation implies that the surface topography may play a dominant role in controlling the protein adsorption. More obvious trend was observed in Figure 4.17 for the case of multilayer films prepared in the presence of 1M NaCl. A marked increase in protein adsorption as the number of deposition was increased despite the

alternate surface charge. This result supports the speculation on the influence of surface topography.

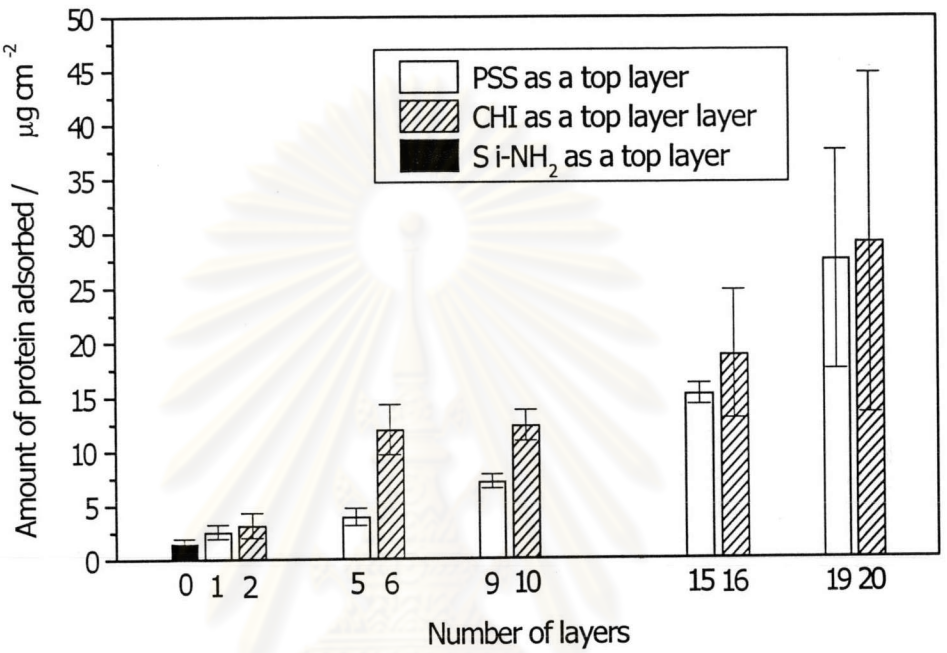

Figure 4.17 The amount of plasma protein adsorption per surface area ($\mu g/cm^2$) of Si-NH_2-(PSS-CHI)$_n$ assemblies prepared in the presence of 1 M NaCl.

Platelet Adhesion

It is well known that platelets also contribute to the thrombus formation. In general, a foreign substrate induces adhesion and activation of platelets with the adsorbed protein layer serving as a controlling factor of the platelet response. Figure 4.18 shows SEM micrographs of Si-NH_2, and multilayer film surfaces prepared in the absence of NaCl after contacting with PRP. Eventhough the trend of protein adsorption was alternate, the responses of platelet adhesion of the supported films having 1-6 layers were not significantly different from the Si-NH_2 substrate. A small number of platelets were randomly appeared on the surfaces of deposited films. We explain this outcome as a consequence of relatively thin individual layer (~ 8 Å) and

overall thickness (~ 8-48 Å). The slight difference in the amount of protein adsorption of such a thin film was not enough to alter the platelet response. It was plausible that each individual layer was not completely covered. The amino groups of the substrate might be visible and thus influence the subsequent platelet response. The reverse effect was observed on the surfaces of Si-NH_2-(PSS-CHI)$_4$-PSS (9 layers) and Si-NH_2-(PSS-CHI)$_5$ (10 layers) whose overall thicknesses were 77 and 89 Å, respectively. It should be noted that these two surfaces have a similar surface roughness. The platelet response was solely determined by the nature of surface charge. Platelets were completely absent on the surface of Si-NH_2-(PSS-CHI)$_4$-PSS whereas quite a few platelets were adhered on Si-NH_2-(PSS-CHI)$_5$. The reversed trend seemed to disappear on the surfaces having 15-20 deposited layers. A large number of platelet adhesion was observed regardless of its alternate surface charge. These data agree well with the protein adsorption and support the speculation on the influence of surface topography. There were no direct correlation between the amount of protein adsorbed and the number of platelet adhered in this particular case. Although the number of adhered platelets continued increasing as a function of number of deposition, the amount of adsorbed protein was only varied in a narrow range of 5-10 $\mu g/cm^2$. This observation also implied that the platelet response was not only dictated by the amount of adsorbed protein but also by the topography of the surface. The adhesion of platelet whose molecule had a diameter of 2-3 μm (much larger than regular plasma proteins) was much more sensitive to the surface topography considering both R_a and R_z values.

Since much thicker individual layer can be formed in the presence of 1M NaCl, the alternate response of platelet was observed even on Si-NH_2-PSS and Si-NH_2-(PSS-CHI) assemblies. The platelets seem to adsorb more on positively charged surfaces with CHI as a top layer. The opposite trend was observed when the surface charge became negative having PSS as the top layer. This indicated that each individual layer was thick enough and the response was directed by the top layer. We found that when the number of deposition increased to 15, the alternate activity was no longer observed. Once again, this can be regarded as a consequence of the surface becoming rougher as the number of deposition increases.

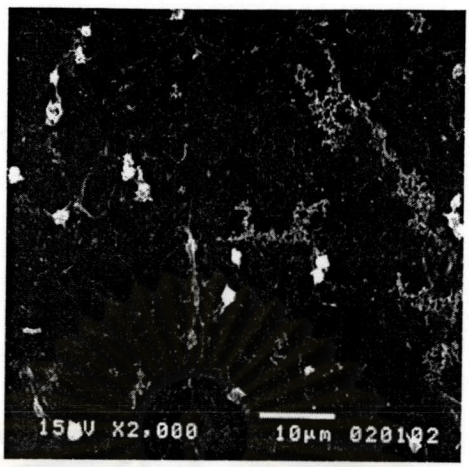

(a) Si-NH_2 layer

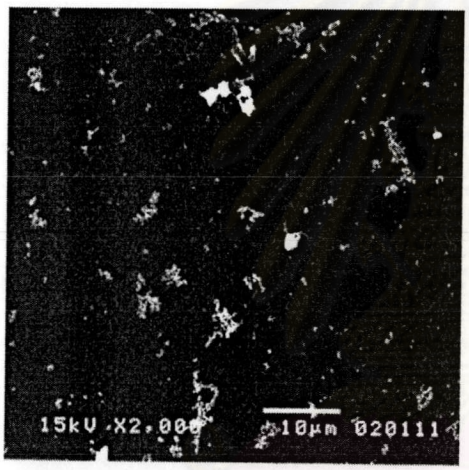

(b) Si-NH_2-PSS (1 layer)

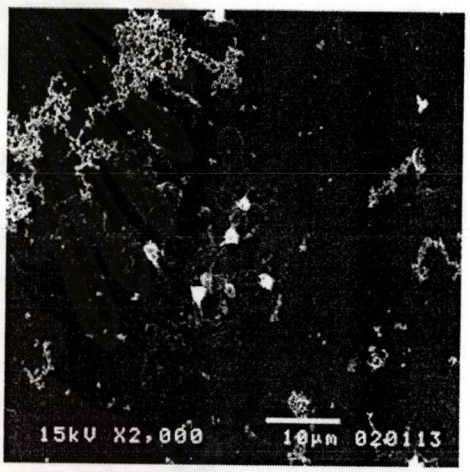

(c) Si-NH_2-(PSS-CHI) (2 layers)

(d) Si-NH_2-$(PSS\text{-}CHI)_2$-PSS (5 layers)

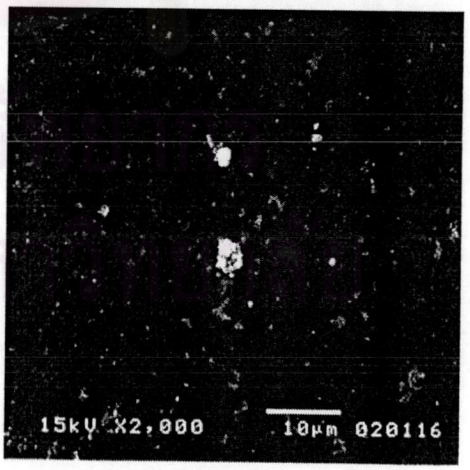

(e) Si-NH_2-$(PSS\text{-}CHI)_3$ (6 layers)

Figure 4.18 SEM micrographs of Si-NH_2-$(PSS\text{-}CHI)_n$ assemblies prepared in the absence of NaCl after contact with PRP.

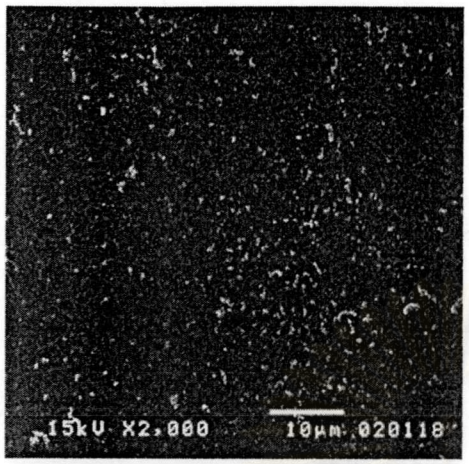

(f) Si-NH_2-(PSS-CHI)$_4$-PSS (9 layers)

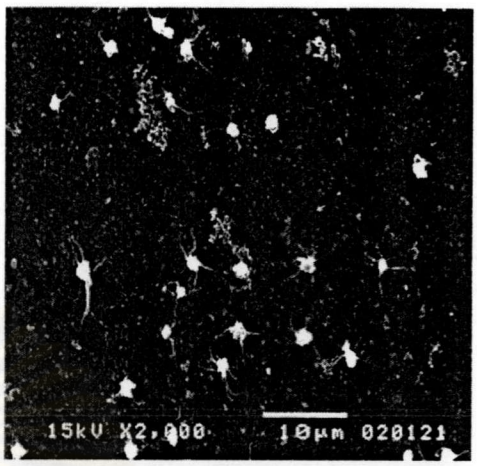

(g) Si-NH_2-(PSS-CHI)$_5$ (10 layers)

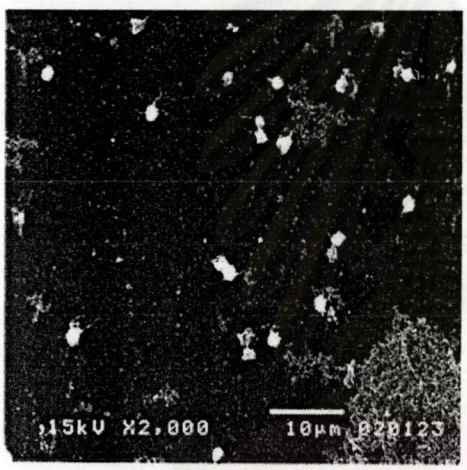

(h) Si-NH_2-(PSS-CHI)$_7$-PSS (15 layers)

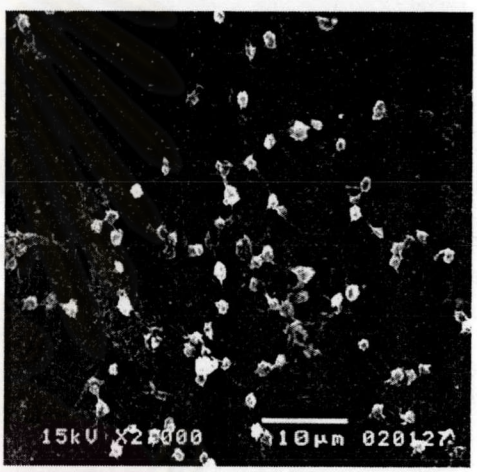

(i) Si-NH_2-(PSS-CHI)$_8$ (16 layers)

(j) Si-NH_2-(PSS-CHI)$_9$-PSS (19 layers)

(k) Si-NH_2-(PSS-CHI)$_{10}$ (20 layers)

Figure 4.18 (continued)

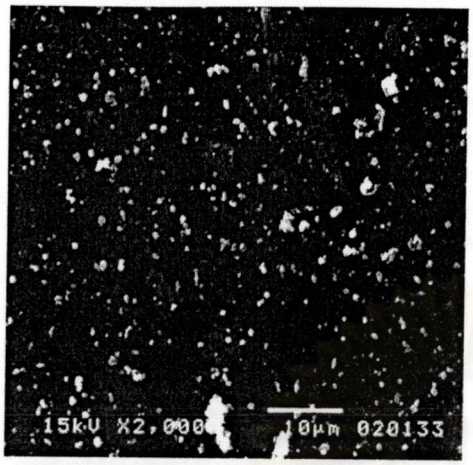

(a) Si-NH_2-PSS (1 layer)

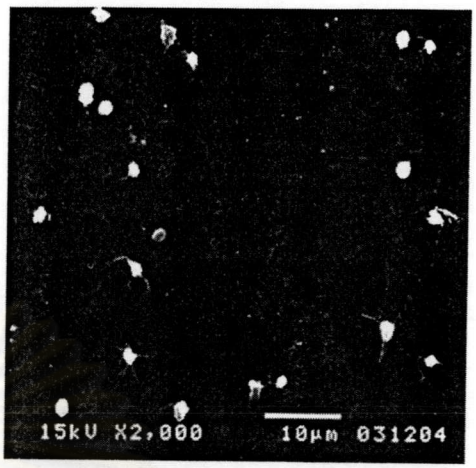

(b) Si-NH_2-(PSS-CHI) (2 layers)

(c) Si-NH_2-(PSS-CHI)$_2$-PSS (5 layers)

(d) Si-NH_2-(PSS-CHI)$_3$ (6 layers)

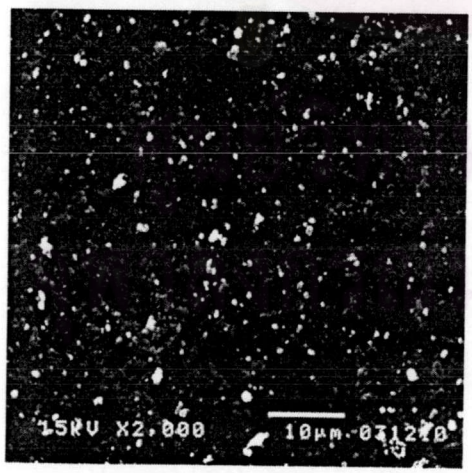

(e) Si-NH_2-(PSS-CHI)$_4$-PSS (9 layers)

(f) Si-NH_2-(PSS-CHI)$_5$ (10 layers)

Figure 4.19 SEM micrographs of Si-NH_2-(PSS-CHI)$_n$ assemblies prepared in the presence of 1 M NaCl after contact with PRP.

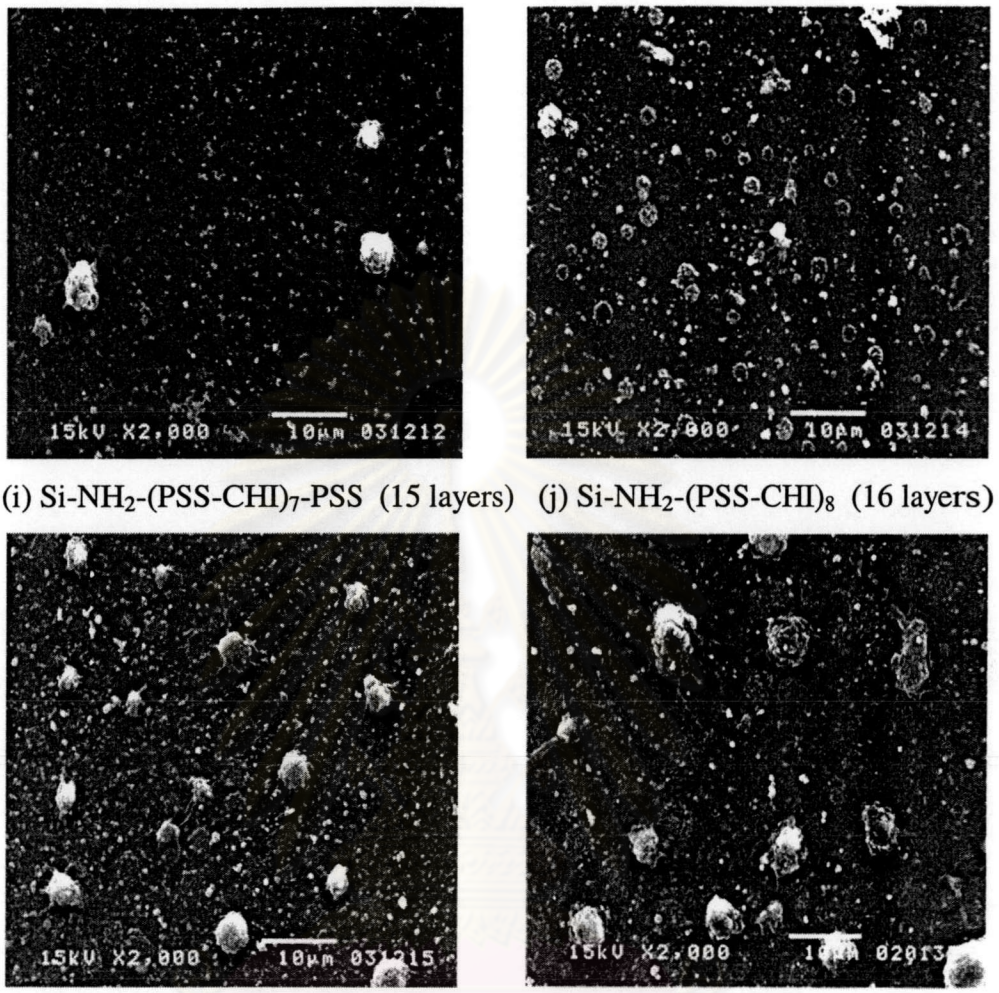

(i) Si-NH_2-(PSS-CHI)$_7$-PSS (15 layers) (j) Si-NH_2-(PSS-CHI)$_8$ (16 layers)

(k) Si-NH_2-(PSS-CHI)$_9$-PSS (19 layers) (l) Si-NH_2-(PSS-CHI)$_{10}$ (20 layers)

Figure 4.19 (continued)

Although there were no platelets adhered to Si-NH_2-PSS, Si-NH_2-(PSS-CHI)$_2$-PSS and Si-NH_2-(PSS-CHI)$_4$-PSS assemblies, we noticed that there were small particulates randomly distributed throughout the surface. We were still uncertain whether or not they were NaCl aggregation. Interestingly, it was obvious that the platelets became highly aggregated when the surfaces became really rough (high R_a and R_z). The result of platelet activity only corresponded quite well with the protein adsorption on surfaces having 5-20 layers.